

Chapter 24

ANFIS-Based Prediction Model for Tool Wear Criteria During Orbital Electrical Discharge Machining of Ti6Al4V



Naisarg H. Sagathiya , Ashish R. Prajapati , Keyur P. Desai, and Harshit K. Dave 

Introduction

Since World War II, to address the growing list of industrial requirements, researchers have developed number of nontraditional machining processes. Electrical discharge machining (EDM) is a versatile nontraditional material removal process in which it is possible to machine any shaped cavity using a tool having the same shape that of the desired cavity. In EDM, both the work material and the tool are needed to be conductors of electricity, and both of them are submerged in a dielectric medium. Initiation of discharges is created by applying high voltage difference between the workpiece and tool, overcoming the breakdown strength of the dielectric fluid at the small gap between the two materials. A small channel of plasma is formed in the gap and expands further with discharge duration [1]. This plasma channel creates an extremely high temperature, which eventually melts and evaporates material from both the tool and workpiece.

In EDM, the size of the hole machined will always be greater than that of the tool, which is called as overcut. Overcut in EDM cannot be eliminated. It can be minimized by selecting the optimum input parameters. Minimization of overcut also endures the problem of flushing and removal of solidified partials from hole cavity. This problem can be rectified by using orbital movement of the tool. It increases clearance gap between the electrode and the hole, which helps in flushing the dielectric fluid to the bottom of the hole, which ultimately improves flushing. Also, the shape of the electrical discharge machined cavity dramatically depends on the shape and size of the tool electrode [2]. It is not possible for a single size tool to machine cavity of different sizes. So, to machine different sizes of hole using a single size tool, orbital

N. H. Sagathiya · A. R. Prajapati (✉) · K. P. Desai · H. K. Dave
Department of Mechanical Engineering, S. V. National Institute of Technology, Surat 395007,
India
e-mail: [iamarp5155@gmail.com](mailto:iamp5155@gmail.com)

EDM is used. Orbital tool movement in EDM process is used to detach the size of the electrode from the size of the hole to be machined. Hence, the standard the size electrode from the market can be utilized to machine a hole of size bigger than the electrode.

Tsai and Wang [3] did a comparative analysis of six neural networks and ANFIS models to predict the material removal rate (MRR). They concluded that ANFIS model gave the best results with a 16.33% error. Mandal et al. [4] have used ANN to model the electrical discharge machining process. They predicted the values of MRR and TWR utilizing those models. Pradhan et al. [5] have studied two artificial intelligent models, namely radial basis function neural network (RBFN) and back propagation neural network (BPN) to predict the surface roughness of electrical discharge machined parts of AISI D2 steel. They observed that both the methods gave satisfactory results and the difference between the predicted and experimental values by both the methods found lower. Markopoulos et al. [6] have predicted the surface roughness of EDMed parts of different steel grades using ANN. Gao et al. [7] have studied the four different algorithms of ANN to predict the MRR and TWR. They observed that the Levenberg Marquardt algorithm (LM) gave minimum error while predicting the values selected response parameters. Caydas et al. [8] have used ANFIS to anticipate the thickness of white layer (WLT) and surface roughness values of wire-ED machined surface. They made a model with reasonable difference between experimental and predicted values. Rao et al. [9] carried out experiments on M-250, HE15, Ti6Al4V and 15CDV6 materials machined with EDM process. They developed models for surface roughness using ANN along with or without the genetic algorithm (GA). They found that the model designed using ANN with GA gave lower error compared to other model. Maji et al. [10] have developed the models of ANFIS using linear and nonlinear membership functions (MFs) to predict the MRR and surface roughness values. They concluded that using nonlinear membership functions, models gave slightly better results.

Dave et al. [11] have studied the EDM of nickel-based alloy under orbital tool movement using Taguchi L25 orthogonal array. They found out the most significant variables affecting MRR and surface roughness are pulse on time and current. Prabhu et al. [12] studied the modeling of carbon nanotube (CNT)-based EDM of tool steel D2 using ANFIS mathematical approach. They predicted the surface roughness of parts machined with and without CNT mixed dielectric with acceptable errors. Al-Ghamdi et al. [13] made the relationship between EDM parameters and MRR using five ANFIS models with 51, 6, 9, 19 and 21 rules and found that model with 21 and 9 runs gave better results. Mathai et al. [14] have studied the effects of EDM parameters on end wear of the tool. They carried out experiments on Ti6Al4V alloy using copper electrode of square cross-section. They found out that pulse ON time affects the most on tool wear characteristics. Hourmand et al. [15] worked on nanopowder mixed EDM of a metal matrix composite Al-Mg₂Si material. They used ANFIS model to predict the MRR. From ANFIS model, they observed that the interaction of voltage–current and pulse on time–current has the highest effects on MRR. Dave [16] has applied PSO (particle swarm optimization) and TLBO (teaching learning-based optimization) techniques on orbital path EDM process to get the optimized

(maximum) values of MRR of the Nickel alloy and ANSI 304 steel materials. He found that TLBO technique generated higher value of MRR compared with PSO even by using less number of iterations.

Several authors have developed models creating relation between input–output parameters of die-sinking EDM and wire EDM using ANFIS and other modeling techniques. However, no work has been reported on the modeling of orbital EDM process on Ti6Al4V alloy using copper tool utilizing ANFIS technique. In the present study, ANFIS models have been developed to establish relationship between orbital EDM parameters, which are orbital radius, orbital speed, current, pulse on time and duty factor with response parameters, namely tool wear rate and tool end wear.

Adaptive Neuro-Fuzzy Interface System (ANFIS)

Fuzzy modeling, initially developed by Takagi and Suguno has found number of applications in the prediction, interface and control. ANFIS is one of the most frequently used fuzzy interface systems, especially in practical applications. ANFIS was originally proposed by Jang in 1993 after which it has been modified according to modern needs. ANFIS generates a relationship between input and output by combining fuzzy logic tool and ANN. Fuzzy logic does not have any predefined technique for conversion, and it takes longer time to cope up with the membership functions (MFs). However, ANN has better learning capacity to accommodate with environment. Thus, ANN is combined with fuzzy logic to cop up with fuzzy logic MFs.

A fuzzy interface system has three essential components, which are based on the “If-Then” rule, technique interface and fuzzy set membership. A detailed view of FIS is given in Fig. 24.1. FIS changes the given value into fuzzy value with the help of membership functions, which has values between 0 and 1. Basic components of knowledge base are database and rule base for generating the results [17].

The adaptive network is a multilayer feed-forward neural network. The basic diagram of adaptive network is composed of number of interconnected nodes. Every node performs a particular function on incoming function coming to the node. By selecting the proper learning method, the error of the output can be reduced. ANFIS

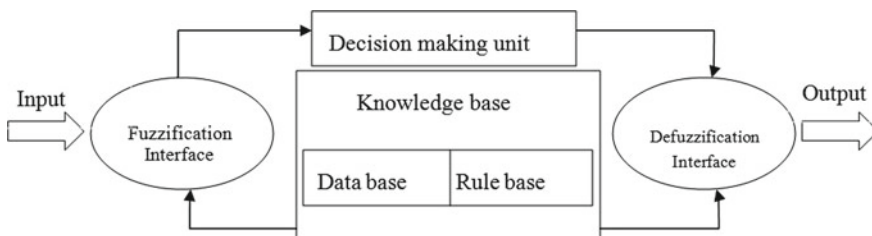


Fig. 24.1 Fuzzy interface system (FIS)

provides two optimization methods, namely, back propagation and hybrid. Basic back propagation algorithm has some limitation of slow convergence, which always tends to stay local. Because of this limitation of back propagation algorithm, a hybrid learning algorithm has been used in this study.

ANFIS Architecture

ANFIS architecture is made of five network layers and the hybrid algorithm has been used to train system based on the input–output data. Takagi and Sugeno’s diagram of ANFIS, which has two input parameters (x and y) and one output function (z) with two membership functions (MFs) are shown in Fig. 24.2. Two fuzzy rules (If-Then) of first-order Sugeno modes are given below:

$$\text{Rule 1 : If } x \text{ is } A_1 \text{ and } y \text{ is } B_1 \text{ Then } f_1 = p_1 x + q_1 y + r_1 \tag{24.1}$$

$$\text{Rule 2 : If } x \text{ is } A_2 \text{ and } y \text{ is } B_2 \text{ Then } f_2 = p_2 x + q_2 y + r_2 \tag{24.2}$$

where, A_1, A_2, B_1 and B_2 are input functional parameters, and p_1, q_1, r_1, p_2, q_2 and r_2 are output functional parameters.

All the layers of ANFIS model, which are shown in Fig. 24.2, are described below:

Layer 1: In this fuzzification layer, each input is the adaptive node that transformed into linguistic with the help of MFs. Every node (i) in this layer is the square node with a node function as:

$$O_i^1 = \mu_{A_i}(x), \tag{24.3}$$

where, $i = 1, 2$ and μ_{A_i} is a degree of membership functions for input x

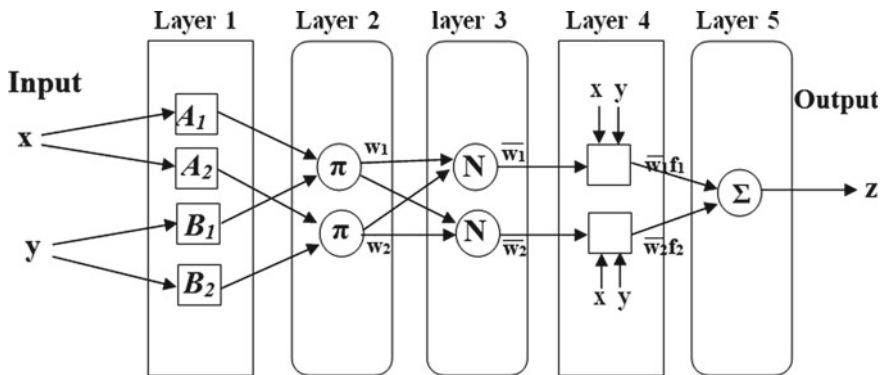


Fig. 24.2 ANFIS architecture

Layer 2: Each node in this layer is a circular node, which multiplies the incoming signal and sends data out. In this layer, each node is a nonadaptive type. It can be given as below:

$$\omega_i = \mu_{A_i}(x)\mu_{B_i}(y), i = 1, 2 \quad (24.4)$$

Layer 3: Each node in this layer in circular shape is labeled with N , and all of them are fixed. It represents the firing strength from layer 2. Firing strength can be calculated as below:

$$\bar{\omega}_i = \frac{\omega_i}{\omega_1 + \omega_2}, i = 1, 2 \quad (24.5)$$

Layer 4: This is a defuzzification layer, which is adaptive. Each node (i) in this layer is a square node with function:

$$\bar{\omega}_i f_i = (p_i x + q_i y + r_i) \quad (24.6)$$

where, ω_i is the output from layer 3, and $(p_i x + q_i y + r_i)$ is called as consequent parameter.

Layer 5: This single node layer is the output layer, which is modeled by ANFIS. It is shown in a circular shape and labeled as Σ , that is overall output by summation of all incoming output:

$$\sum_i \bar{\omega}_i f_i = \frac{\sum_i \omega_i f_i}{\sum_i \omega_i}, \quad (24.7)$$

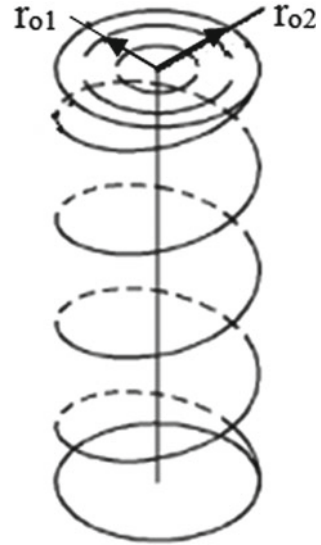
From the above ANFIS model, a relationship between input and output values can be successfully established using different combinations of MFs, rule bases and other parameters from the loaded database.

Experimental Plan and Procedure

Machine Setup

In the present study, Titanium superalloy Ti6Al4V as a workpiece is selected for the experimentation. Ti6Al4V material has an excellent combination of toughness, strength, corrosion-resistance and high strength to weight ratio. Copper with positive polarity is taken as a tool electrode material of 9 mm diameter. The size of the workpiece is 15 mm × 15 mm × 10 mm, in which a hole of depth 4 mm of different diameter was generated. Single diameter tool is used to drill the holes of five different

Fig. 24.3 Helical tool movement path



diameters. Standard EDM oil has been chosen as a dielectric fluid in the present experiments.

Joemars JM322 EDM machine is used in the study. It is equipped with orbital cutting attachment, which can be utilized for boring operation. With the orbital motion of tool, it can be possible to disassociate the size of the cavity with that of the tool. In these experiments, helical movement of the tool is selected, in which tool moves simultaneously in all three axes x , y and z in helical path, which is illustrated in Fig. 24.3. As shown in Fig. 24.4a, workpiece is fixed in workpiece fixture and electrode tool held in tool holder. Side flushing has been used, in which dielectric fluid jet of 1 bar pressure was directed towards the sparking area through a nozzle. Condition of tool and workpiece after machining can be observed in Fig. 24.4b. After the completion of machining, both the tool and workpiece were thoroughly cleaned using acetone and placed on ultrasonic vibrator to remove the carbon soot from the tool and workpiece surfaces and then dried using tissue paper to remove the remaining oil stain.

Experimental Design

Total five input parameters, namely orbital speed (S_o^-), orbital radius (r_o), duty factor (DF), pulse ON time (t_{ON}) and current (I) are selected with five levels for each parameter. Values of all the selected parameters are chosen as the difference between two values remains nearly same. The values of each level for all selected parameters are given in Table 24.1. The following experiment is designed with Taguchi's L25 orthogonal array as there are total five input parameters and five levels for each

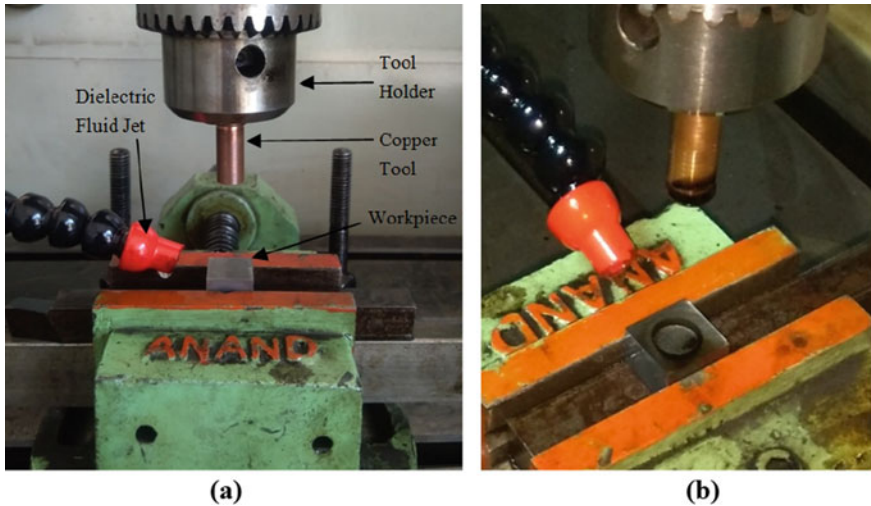


Fig. 24.4 a Machining setup, b Tool and W/P condition after machining

Table 24.1 selected parameters along with their levels

| Parameter | P1 | P2 | P3 | P4 | Unit |
|----------------------------|------|------|------|------|---------|
| Orbital radius (r_o) | 0.4 | 0.8 | 1.2 | 1.6 | mm |
| Orbital speed (S_o) | 0.05 | 0.07 | 0.09 | 0.11 | mm/s |
| Current (I) | 9 | 13 | 17 | 21 | A |
| Pulse ON time (t_{ON}) | 93 | 165 | 240 | 315 | μ s |
| Duty factor (DF) | 0.4 | 0.5 | 0.6 | 0.7 | – |

parameter. In this design, there are total 25 rows. All the experiments have been done twice for precise evaluation of results. So, total 50 workpieces and tools have been prepared for experimentation.

Two response characteristics, TWR and tool end wear were selected for ANFIS modeling. To calculate the TWR, weights of the tool before and after machining were measured using Citizen made precision electronic weighing machine having resolution of 0.001 gm. Then, the weights are converted into volume by using density of the tool material. Machining time is counted using precision watch having resolution of 1 s. TWR (mm^3/min) has been calculated by utilizing the following equation:

$$\text{TWR} = \frac{(T_{wi} - T_{wf})}{\rho_T \times t} \tag{24.8}$$

where

T_{wi} Initial weight of the tool (gm)

T_{wf} Final weight of tool (gm)
 ρ_T density of tool material (gm/mm³)
 t machining time (min)

Tool end wear (mm) is a change in the length of the tool before and after machining. It was measured in the EDM machine itself with 0.001 mm precision. The following equation can calculate the tool end wear:

$$\text{End wear } \Delta l_T = l_{T_i} - l_{T_f} \quad (24.9)$$

where, l_{T_i} is the length of the tool before machining and l_{T_f} is the maximum length of the tool after machining.

Result and Discussion

As discussed in the earlier section, Taguchi's L25 orthogonal array design is selected for experimentation, and all the experiments were done twice. The average of these two result data is used in the modeling process. Result data of both the chosen response parameters with Taguchi's L25 design are given in Table 24.2. From the result table, it can be seen that the highest values of tool wear criteria are found during experiment number 9.

ANFIS Model for TWR and Tool End Wear

ANFIS model was developed in MATLAB Mathwork software. The neuro-fuzzy tool available in this software was used to structure ANFIS. In the present study, 80% of the experimental data (20 experiments) were selected randomly for the training process and 20% of data (five experiments) for testing purpose. It means that five results for both the selected responses were predicted using ANFIS model and then compared with experimental results. Sugeno type fuzzy interface system with hybrid learning algorithm is utilized for the modeling of both the response parameters.

In the ANFIS structure generated by the software have five input parameters with one output parameter. In third layer, a total of 20 rules were used for the prediction of the output values. In layer 1, fuzzification of input parameters takes place to 20 membership function in layer 2. To make a model, first, it is needed to call the training data in the ANFIS work system. These data help in searching the constant of the membership function. In the present study, subtractive clustering fuzzy interface system has been selected. Parameters of the subtractive clustering technique used in this study are given in Table 24.3. These ANFIS variables have been optimized after a number of tests.

Table 24.2 Experimental design and results of TWR and tool end wear

| Exp. | Orbital radius (mm) | Orbital speed (mm/s) | Current (A) | Pulse ON time (μs) | DF | TWR (mm ³ /min) | Tool end wear (mm) |
|------|---------------------|----------------------|-------------|--------------------|-----|----------------------------|--------------------|
| 1 | 0.4 | 0.05 | 9 | 93 | 0.4 | 0.036 | 0.271 |
| 2 | 0.4 | 0.07 | 13 | 165 | 0.5 | 0.057 | 0.199 |
| 3 | 0.4 | 0.09 | 17 | 240 | 0.6 | 0.0985 | 0.271 |
| 4 | 0.4 | 0.11 | 21 | 315 | 0.7 | 0.102 | 0.183 |
| 5 | 0.4 | 0.13 | 28 | 385 | 0.8 | 0.171 | 0.307 |
| 6 | 0.8 | 0.05 | 13 | 240 | 0.7 | 0.0428 | 0.135 |
| 7 | 0.8 | 0.07 | 17 | 315 | 0.8 | 0.0542 | 0.149 |
| 8 | 0.8 | 0.09 | 21 | 385 | 0.4 | 0.0836 | 0.259 |
| 9 | 0.8 | 0.11 | 28 | 93 | 0.5 | 0.8146 | 1.108 |
| 10 | 0.8 | 0.13 | 9 | 165 | 0.6 | 0.0299 | 0.195 |
| 11 | 1.2 | 0.05 | 17 | 385 | 0.5 | 0.0656 | 0.249 |
| 12 | 1.2 | 0.07 | 21 | 93 | 0.6 | 0.2529 | 0.811 |
| 13 | 1.2 | 0.09 | 28 | 165 | 0.7 | 0.2448 | 0.584 |
| 14 | 1.2 | 0.11 | 9 | 240 | 0.8 | 0.0138 | 0.057 |
| 15 | 1.2 | 0.13 | 13 | 315 | 0.4 | 0.0309 | 0.225 |
| 16 | 1.6 | 0.05 | 21 | 165 | 0.8 | 0.1235 | 0.452 |
| 17 | 1.6 | 0.07 | 28 | 240 | 0.4 | 0.2352 | 0.646 |
| 18 | 1.6 | 0.09 | 9 | 315 | 0.5 | 0.0155 | 0.154 |
| 19 | 1.6 | 0.11 | 13 | 385 | 0.6 | 0.0416 | 0.223 |
| 20 | 1.6 | 0.13 | 17 | 93 | 0.7 | 0.1251 | 0.558 |
| 21 | 2 | 0.05 | 28 | 315 | 0.6 | 0.2307 | 0.613 |
| 22 | 2 | 0.07 | 9 | 385 | 0.7 | 0.0182 | 0.13 |
| 23 | 2 | 0.09 | 13 | 93 | 0.8 | 0.0657 | 0.531 |
| 24 | 2 | 0.11 | 17 | 165 | 0.4 | 0.095 | 0.596 |
| 25 | 2 | 0.13 | 21 | 240 | 0.5 | 0.1365 | 0.587 |

The data are trained using hybrid optimization method with 50 epochs. ANFIS then calculated the error between input values and the predicted values generated from the model.

Model Performance for the Prediction of Tool Wear Rate and Tool End Wear

As in the present research, Taguchi’s L25 experimental design is used; there are total 25 output readings. Out of which 20 data were selected randomly for training

Table 24.3 ANFIS criteria used in creating the model

| Criteria | Descriptor/values |
|---------------------------------------|-------------------------------|
| FIS structure | Sugeno subtractive clustering |
| Number of training and testing data | 20 and 5 |
| Reject ratio | 0.15 |
| Squash factor | 1.25 |
| Accept ratio | 0.1 |
| Range of influence | 0.5 |
| Number of outputs | 1 |
| Number of inputs | 5 |
| Optimization method | Hybrid |
| Numbers of input membership functions | 20 20 20 20 20 |
| Number of training epochs | 50 |

the model. The remaining five data were used for the prediction of both the output parameters. The error between experimental values and predicted value has been evaluated by statistical equations. ANFIS model performance is evaluated by using statistical functions, namely root mean square error (RMSE) and mean absolute error (MAE). Equations for these functions are given below:

$$MAE = \frac{1}{n} \sum_{t=1}^n |P_t - E_t| \tag{24.10}$$

$$RSME = \sqrt{\frac{\sum_{t=1}^n (P_t - E_t)^2}{n}} \tag{24.11}$$

where, P_t is predicted result from ANFIS, E_t is experimental result, and n is the total number of data selected for the calculation of error.

The lower value of RSME indicates the better predictability of the model. As it can be observed from Table 24.4 that model for tool wear rate gave smaller error than the model for the tool end wear. While measuring the tool end wear, the taper on the tool was not considered, this is nullified in the calculation of TWR. The predicted and experimental values of both TWR and tool end wear in graphical form are shown in Fig. 24.5a, b, respectively.

Table 24.4 Errors of predicted result

| Response characteristic | MAE | RSME |
|-------------------------|---------|---------|
| Tool wear rate | 0.01164 | 0.01415 |
| Tool end wear | 0.0396 | 0.04583 |

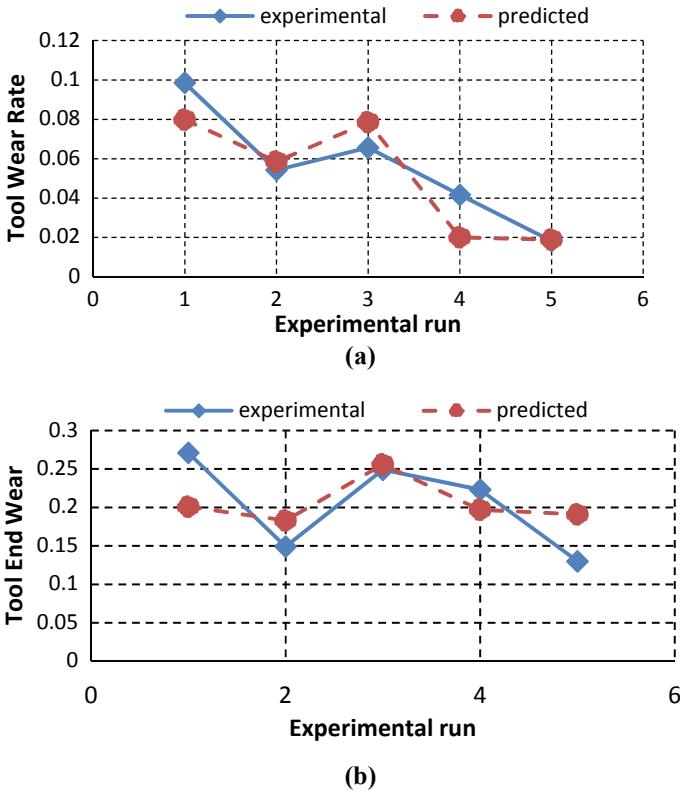
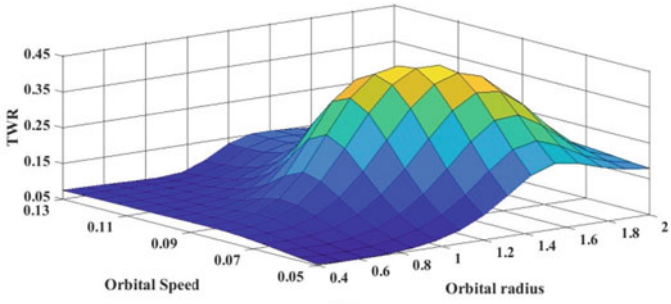


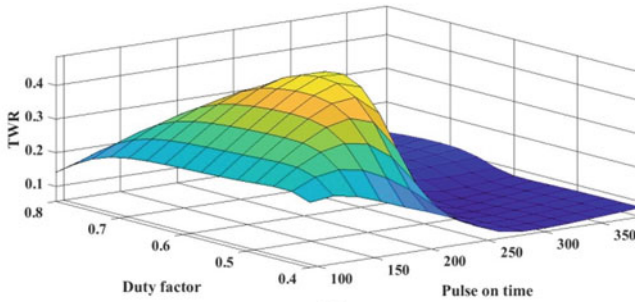
Fig. 24.5 Comparative diagram of experimental and predicted values through ANFIS for **a** TWR and **b** Tool end wear

From Fig. 24.5a, it can be seen that two predicted values (experimental runs 1 and 4) have a relatively larger error for tool wear rate than other experimental runs. Error for two predicted values (experimental runs 2 and 5) has minimum error compared with others. In the case of the tool end wear also errors found higher for two values (experimental runs 1 and 5), which can be observed in Fig. 24.5b. While the experimental run 3 has the lowest error. Thus, ANFIS model can be used for generating a model with minimum values of error.

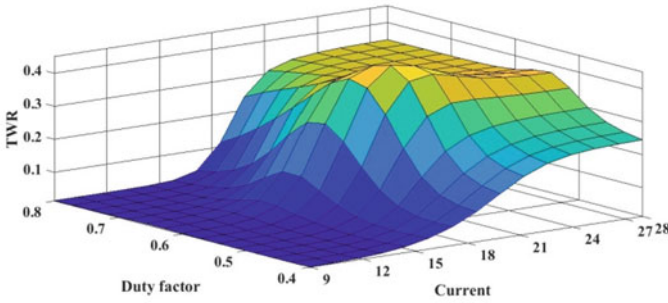
Moreover, ANFIS has generated nonlinear surface plots of response variable against two input variables. Some of the selected surface graphs of two input parameters with TWR and tool end wear are shown in Figs. 24.6 and 24.7, respectively. TWR and tool end wear found larger at the high orbital radius values (Figs. 24.6a and 7a). From Fig. 24.6b, it can be observed that tool wear rate decreases with an increase in t_{ON} . Also, from Fig. 24.6c, TWR is found increasing with an increase in current values. Figure 24.6b indicates that, at lower pulse on time values, tool end wear is more significant compared with higher values. By observing Fig. 24.7b, it can be said that the tool end has worn significantly when the lower machining time



(a)



(b)



(c)

Fig. 24.6 Change in tool wear rate with respect to **a** orbital speed (S_o) and orbital radius (r_o), **b** Duty factor and Pulse on time and **c** Duty factor and current

was used. Referring to Fig. 24.7c, tool end wear is found to be increasing with an increase in current and duty factor values.

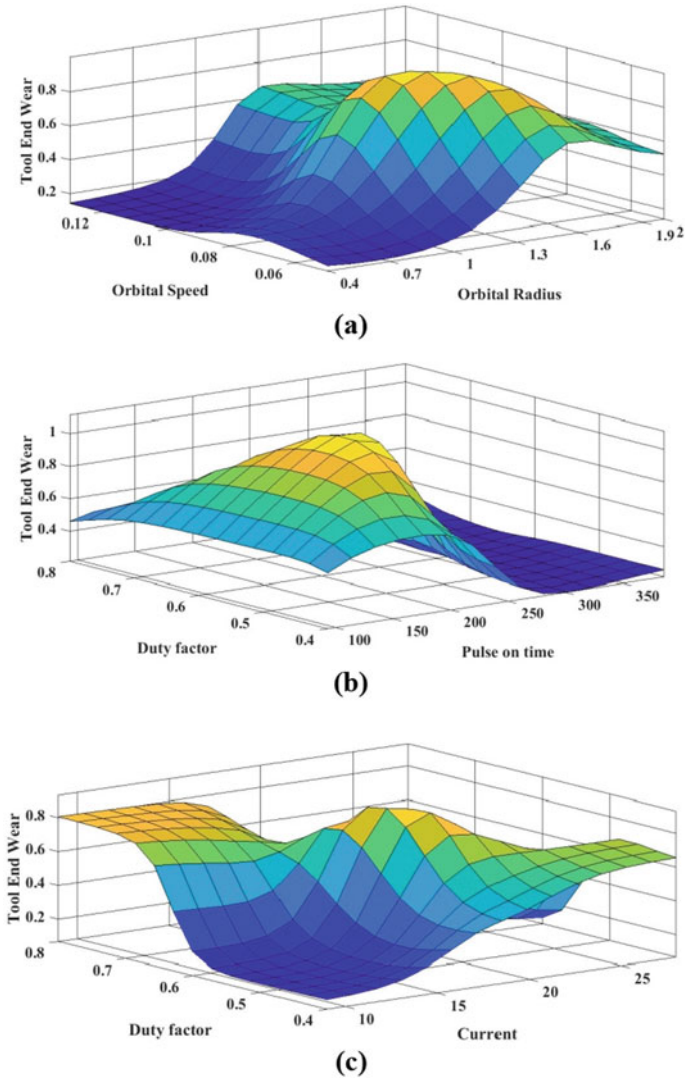


Fig. 24.7 Change in tool end rate with respect to **a** orbital speed (S_o) and orbital radius (r_o), **b** Duty factor and Pulse on time and **c** Duty factor and current

Conclusion

Orbital tool movement in EDM helps in drilling the hole of different diameters with a single diameter tool. In the present research work, models for tool wear rate and tool end wear were successfully developed using ANFIS. The developed model helped in predicting the values of responses with reasonable errors. Error predicted for tool

end wear was found higher than the error anticipated for tool wear rate. Results show an increasing trend on tool wear characteristics with an increase in the current values. Also, tool wear characteristics were found lower at higher pulse on time and lower orbital radius. It can be concluded that with the help of the surface graphs, prediction of the behavior of responses because of a change in the independent parameters can be easily generated through ANFIS. Thus, ANFIS modeling can be utilized for process planning to predict the tool wear prior to the machining initiation.

References

1. Kunieda M, Lauwers B, Rajurkar KP, Schumacher BM (2005) Advancing EDM through fundamental insight into the process. *CIRP Ann* 54(2):64–87
2. Benedict GF (1987) *Nontraditional manufacturing processes*. CRC Press, vol 19
3. Tsai KM, Wang PJ (2001) Predictions on surface finish in electrical discharge machining based upon neural network models. *Int J Mach Tools Manuf* 41(10):1385–1403. <https://doi.org/10.18178/ijmmm.2017.5.3.309>
4. Mandal D, Pal SK, Saha P (2007) Modeling of electrical discharge machining process using back propagation neural network and multi-objective optimization using non-dominating sorting genetic algorithm-II. *J Mater Process Technol* 186(1–3):154–162. <https://doi.org/10.1016/j.jmatprotec.2006.12.030>
5. Pradhan MK, Das R, Biswas CK (2009) Comparisons of neural network models on surface roughness in electrical discharge machining. *Proc Inst Mech Eng J Eng Manuf* 223(7):801–808
6. Markopoulos AP, Manolakos DE, Vaxevanidis NM (2008) Artificial neural network models for the prediction of surface roughness in electrical discharge machining. *J Intell Manuf* 19(3):283–292. <https://doi.org/10.1007/s10845-008-0081-9>
7. Gao Q, Zhang QH, Su SP, Zhang JH, Ge RY (2008) Prediction models and generalization performance study in electrical discharge machining. *Appl Mech Mater* 12:677–681. <https://doi.org/10.4028/www.scientific.net/AMM.10-12.677>
8. Çaydaş U, Haşçalık A, Ekici S (2009) An adaptive neuro-fuzzy inference system (ANFIS) model for wire-EDM. *Expert Syst Appl* 36(3):6135–6139. <https://doi.org/10.1016/j.eswa.2008.07.019>
9. Rao KRM, Rangajanardhaa G, Hanumantha Rao D, Sreenivasa Rao M (2009) Development of hybrid model and optimization of surface roughness in electric discharge machining using artificial neural networks and genetic algorithm. *J Mater Process Technol* 209(3):1512–1520
10. Maji K, Pratihari DK (2010) Forward and reverse mappings of electrical discharge machining process using adaptive network-based fuzzy inference system. *Expert Syst Appl* 37(12):8566–8574. <https://doi.org/10.1016/j.eswa.2010.05.019>
11. Dave H, Desai K, Raval H (2012) Experimental investigations on orbital electro discharge machining of Inconel 718 using Taguchi technique. *Int J Mod Manuf Technol* 4(1):53–58
12. Prabhu S, Uma M, Vinayagam BK (2013) Adaptive neuro-fuzzy interference system modelling of carbon nanotube-based electrical discharge machining process. *J Brazilian Soc Mech Sci Eng* 35(4):505–516. <https://doi.org/10.1007/s40430-013-0047-5>
13. Al-Ghamdi K, Taylan O (2015) A comparative study on modelling material removal rate by ANFIS and polynomial methods in electrical discharge machining process. *Comput Ind Eng* 79:27–41
14. Mathai VJ, Dave HK, Desai KP (2017) Study on effect of process parameters on end wear of tool electrode during planetary EDM of Ti-6Al-4V. *Int J Mater Mech Manuf* 5(3):159–163
15. Hourmand M, Sarhan AA, Farahany S, Sayuti M (2019) Microstructure characterization and maximization of the material removal rate in nano-powder mixed EDM of Al-Mg₂Si metal

- matrix composite-ANFIS and RSM approaches. *Int J Adv Manuf Technol* 101(9–12):2723–2737. <https://doi.org/10.1007/s00170-018-3130-3>
16. Dave HK (2019) Optimization of orbital electro discharge machining parameters using TLBO and PSO algorithms. *Int J Mod Manuf Technol* 11(2):2067–3604
 17. Jang JS (1993) ANFIS: adaptive-network-based fuzzy inference system. *IEEE Trans Syst Man Cyber* 23(3):665–685